ACS OMEGA

http://pubs.acs.org/journal/acsodf

Article

Influence of Composition and Preparation Conditions on the Structure and Properties of Composite Materials TiO_2-SiO_2/CaO with a Spherical Particle Shape Based on Tokem-200 Cationic Exchange Resins

Vladimir V. Kozik, Lyudmila P. Borilo, Ekaterina S. Lyutova, and Yu-Wen Chen*

Cite This: *ACS Omega* 2021, 6, 21104−21112

Read Online

ACCESS | Metrics & More | Article Recommendations

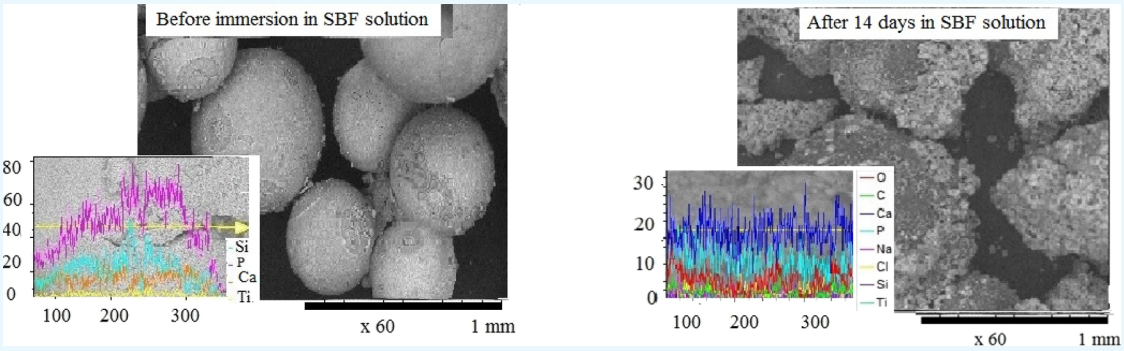

ABSTRACT: Spherical biomaterials based on Tokem-200 cationic exchange resin were synthesized from solutions by the sol−gel method. The material framework is represented by TiO_2-SiO_2, and the inner part is filled with CaO (sample TiO_2-SiO_2/CaO). A stepwise heat treatment (drying at 60 °C) annealing at 150, 250, and 350 °C, each for 30 min, at 600 °C for 6 h, and 800 °C for 1 h is required to obtain a homogeneous material. In simulated body fluid solution, the sample exhibited bioactive properties, and gelatin could be used as a binding additive.

INTRODUCTION

The idea of using artificial materials to replace human organs and tissues has long been known. The main requirements for biomaterials are non-toxicity and high mechanical strength.[1,2] In addition, the implant should retain its functional properties for a certain period of time without significant changes in its structure and mechanical properties.

Great interest in this research has led to the formation of several parallel developing directions: (i) production of dispersed materials, based on synthetic calcium phosphates with its subsequent molding, (ii) development of bioactive glasses, and (iii) development of metal substrates with calcium-phosphate coating.[3−7]

Calcium-phosphate-based materials find many applications in medicine and materials science.[8,9] Calcium-phosphates are used to replace implants in damaged bone tissues (calcium-phosphate cements, coatings, inorganic parts, and composite materials).[10−14] They are able to form a direct biological bond with the living tissue, forming a bone apatite on its surface.[15]

In recent years, calcium-phosphate-based composites modified with silicon and titanium to improve functional characteristics can be considered as a promising material for implants. It was established in many works that the presence of silicon in the calcium-phosphate material accelerates the fusion of the implant and the bone. The crystallite size decreases, and the grain structure of calcium-phosphate materials changes with partial replacement of phosphate groups by the silicate ones. It was found that the osteoinductive properties of calcium-phosphate materials differ significantly depending on the size of macropores with the same chemical composition.[16,17] The size of macropores should be not less than 300 microns, which promotes feeding and spreading of cells on the surface of macropores and formation of capillaries in the implant.[16−21]

Calcium phosphates can be of natural[22−27] or synthetic[3,28,29] origin. It can be obtained using several methods such as aqueous precipitation,[25,29,30] the sol−gel method,[6,30−32] solid

Received: June 3, 2021
Accepted: July 23, 2021
Published: August 4, 2021

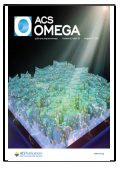

© 2021 The Authors. Published by American Chemical Society

reaction,[33] and hydrothermal method.[34,35] The difficulties of classical liquid-phase methods of calcium phosphate synthesis with a Ca/P ratio ≤1.67 are related to simultaneous monitoring of a large number of factors (temperature, reagent discharge rate, stirring of the reaction mixture, and time) affecting the phase composition, particle homogeneity, and morphology of the synthesis product.[9] Sol−gel synthesis is a promising method of producing biomaterials.[36−39] The properties of the oxide bioactive material produced by sol−gel technology depend on the method of sol preparation and its composition. Using the sol−gel method to obtain sol for the TiO_2-SiO_2 system when forming a sphere shell allows controlling the particle size required to maintain material porosity and provide access for physiological fluids to the entire tissue volume.[36,37]

In recent years, materials containing spherical particles, in particular based on various polymers of up to 0.7 mm in diameter, have been widely used in clinical practice to fill bone defects. Polymeric scaffolds serve as "scaffolds" for living cells that form new bone tissues.[19,38] These scaffolds are made of biodegradable materials: over time, when the bone is already formed, the scaffold material breaks down into simple substances and is removed from the body. Synthetic polymers are the preferred materials for regenerative medicine over the natural ones because they are easier to process and can be adapted to provide a wider range of mechanical properties.[37−41] For the development of a new calcium-phosphate biomaterial with specific physicochemical and functional properties, new opportunities open up when a layered spherical composite with biologically active ions is formed with polymeric composites as a preform. However, the processes of decomposition and excretion of biodegradable materials have not yet been fully studied.

That is why the development of new compositions and physicochemical bases of calcium-phosphate materials production is required to create new materials for regenerative medicine.

The aim of this work was to establish the influence of composition and conditions of production on the structure and properties of the composite materials TiO_2-SiO_2/CaO with the spherical shape of particles on the basis of cationic exchange resins Tokem-200.

RESULTS AND DISCUSSION

Sorption Properties of Cationic Exchange Resins. The choice of cation exchanger for the production of spherical materials was based on the results of studies of the physicochemical properties and selectivity of sorbents to the Ca^{2+} ion.[42] To establish the conditions for producing Tokem-200 with Ca^{2+}, the sorption capacity of Tokem-200 cationic exchange resin to the Ca^{2+} ion under different conditions was studied (Table 1).

Tokem-200 cationite is weakly acidic and has a porous gel structure with an acrylic-divinylbenzene matrix with a carboxyl functional group (sodium form). Heating at 95 °C and microwave exposure increase the mobility of functional groups and thus the sorption of Ca^{2+} ions with Na^+. However, the surface morphology is not affected by heating and microwave exposure (Figure 1a,d,g,b,e,h). According to the results of elemental composition of the surface (Figure 1c,f,i), it was found that no sodium ions were fixed on the surface of the samples after heating (95 °C) and microwave exposure; this indicates a more complete sorption of Na^+ ions onto Ca^{2+} ions.

Table 1. Sorption Capacity of Tokem-200 Cationic Exchange Resin, mmol·eq/g, by the Ca^{2+} Ion

	sorption capacity ±0.06 (mmol·eq/g)
t = 25 °C	8.704
heating on an electric stove (t = 95 °C)	8.711
microwave	
at 264 W and 2 min	8.712
at 264 W and 4 min	8.713
at 440 W and 2 min	8.711

Composition and Properties of Aggregatively Stable Sol. To form a framework of the bioactive material with a spherical shape of particles, an aggregatively stable sol was prepared. Maturation of the sols was carried out at room temperature for 3 days. In the study of the solutions, it was found that, if the silicon oxide content in the solution is high, up to 60 mol %, then the polycondensation catalyst (phosphoric acid) should not be more than 5 mol %. If the acid content is increased in the system, then the solutions become unsuitable for films on the second day. The minimum silicon oxide content in the system should be 30 mol %. Therefore, three compositions were chosen to produce the sol (Table 2).

Figure 2 shows a graph of viscosity versus time for the studied compositions.

The amount of acid in the system was varied for the studied compositions (at 30 mol % silicon oxide content). To obtain uniform coatings, the maximum acid content in the system should be 25 mol %, and the storage time of the solutions is reduced to 5 days.

Orientational interactions prevail for the studied solutions during the first 3 days, so the viscosity of the solutions increases sharply on the second day and decreases on the next day. Subsequently, a new structure is formed in the solutions due to the processes of orientational polarization during the electrostatic interaction of dissolved substances with each other and alcohol molecules.[38,43−45] In the case of a high concentration of phosphoric acid, spatial difficulties are of little importance compared to its catalyzing action, and as a consequence, there is a sharp increase in viscosity at relatively early stages of solution maturation and gelation in the solution.

Orthophosphoric acid increases the acidity of the medium and leads to acceleration of hydrolysis and condensation, so solution 2 was suitable for use up to 6 days, and in solution 3, there was no viscosity stabilization on the fifth day of gelation. Therefore, solution 1 was chosen for further studies. For solution 1, solution stabilization began on the fourth day at a viscosity value of 3.12 mm^2/s.

Thermogravimetric Analysis and IR Spectroscopy. It is possible to distinguish a number of processes occurring during thermal treatment of the obtained materials with a spherical particle shape (Figure 3). At T_{max} = 190 °C (Figure 3a), cationite combustion with formation of water and carbon dioxide occurs. At temperatures above 400 °C, the cationite structure is destroyed, which is accompanied by an exothermic effect at 461 °C.

The decomposition of the cationic-exchanger containing Ca^{2+} (Figure 3b) recorded an additional peak (T_{max} = 542 °C), indicating the formation of CaO. The thermogram of the Tokem-200 cationic-exchanger with Ca^{2+} and applied sol (Figure 3c) did not practically differ from the thermogram of

https://doi.org/10.1021/acsomega.1c02918
ACS Omega 2021, 6, 21104−21112

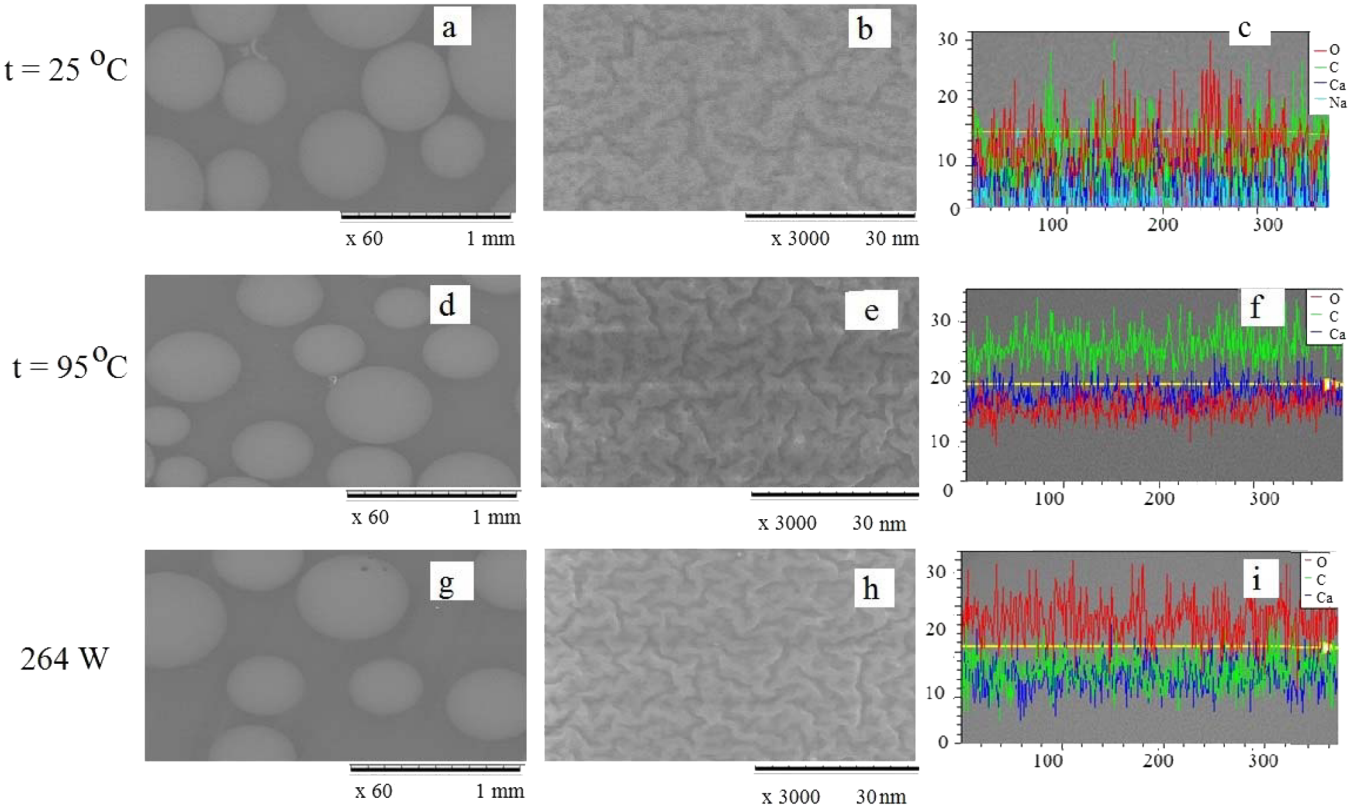

Figure 1. Micrographs of samples Tokem-200 with Ca^{2+} (a, d, g: magnification of 60; b, e, h: magnification of 3000) and distribution of elements along the line (c, f, i).

Table 2. Compositions of Oxide Systems for Obtaining Solutions

	oxide content in the system (mol %)		
number of the train	TiO_2	SiO_2	P_2O_5
1	65	30	5
2	55	30	15
3	45	30	25

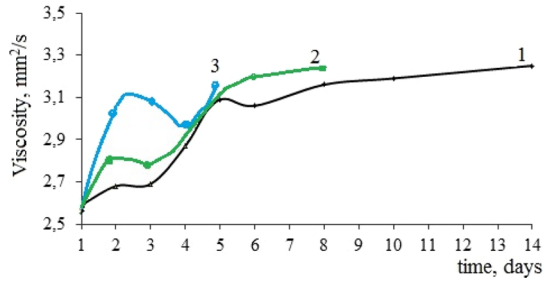

Figure 2. Viscosity as a function of time for formulations: 1. TiO_2-65, SiO_2-30, P_2O_5-5; 2. TiO_2-55; SiO_2-30; P_2O_5-15; 3. TiO_2-45; SiO_2-30; P_2O_5-25 mol %.

Tokem-200 cationic-exchanger decomposition in the absence of sol (Figure 3b) that may be due to the small amount of precipitated sol. Decomposition temperature of the Tokem-200 sample with Ca^{2+} and deposited sol was 600 °C.

Identification of the phases present in the polycrystalline sample was carried out by qualitative X-ray phase analysis. The samples at 600 °C were amorphous. Therefore, it is necessary to increase the temperature treatment up to 800 °C. The $Ca(Si_2O_5)$, CaO, and tridymite phases were detected.

In a previous work,[46] it was found that the structure of the materials was formed by silicon-oxygen and phosphorus-oxygen atomic groups. This is confirmed by the presence of bands at 859−871 cm^{-1} in the IR spectrum, which correspond to stretching asymmetric vibrations of Si−O−Si, stretching symmetric vibrations of Si−O−P, and stretching symmetric vibrations of PO_4.[47] Tensile symmetrical vibrations of the Si−O−Si and P−O−P bonds were detected only at temperature treatments of 600 and 800 °C. Ti−O bond vibrations were identified only at 600 °C. In addition, tetrahedral SiO_4 and PO_4, symmetrical vibrations of Si−O−Ti groups, and symmetrical vibrations of the Si−O−Si bond bridge in the $[SiO_4]$-tetrahedral bond were present in the materials. The absorption bands in the low-frequency region of 400−550 cm^{-1} are associated with bending vibrations of the O−Si−O end bonds and with calcium-oxygen bond vibrations in $[CaO_6]$-octahedron.[44]

Microstructure and Dispersion. To obtain a homogeneous material requires stepwise heat treatment (after drying at 60 °C) at 150, 250, and 350 °C, each lasting 30 min, at 600 °C for 6 h, and at 800 °C for 1 h. Figure 4 shows the microphotographs of the sample after heat treatment.

For the sample obtained by step heat treatment, the framework was uniformly fixed on the cationite, while the sample obtained without step treatment (drying at 60 °C and annealing at 800 °C) had cracks and splits on its surface, which is not favorable for practical applications.

Surface characteristics are important when studying the properties of biomaterials because they depend on vital processes such as protein and cell adhesion and the bioresorbability of materials when implanted into the body. Bioactive properties depend on the charge and porosity of the

https://doi.org/10.1021/acsomega.1c02918
ACS Omega 2021, 6, 21104−21112

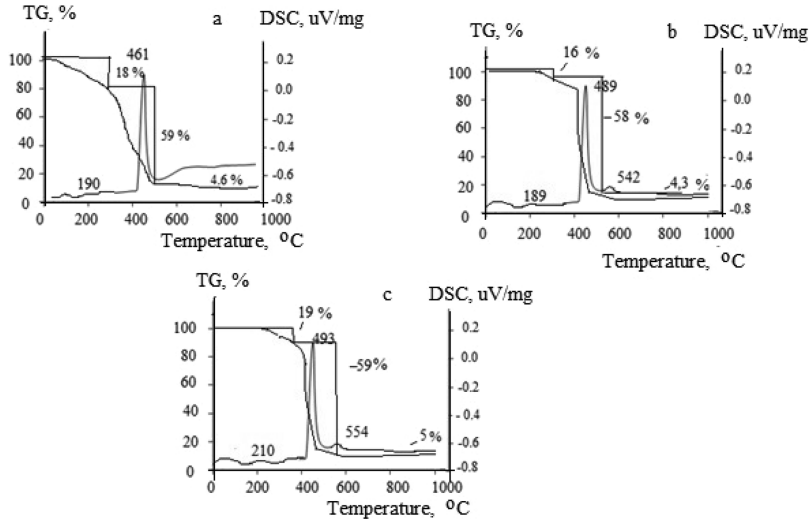

Figure 3. Data of thermogravimetric analysis of samples: Tokem-200 (a), Tokem-200 with Ca^{2+} (b), and Tokem-200 with Ca^{2+} and applied sol (c).

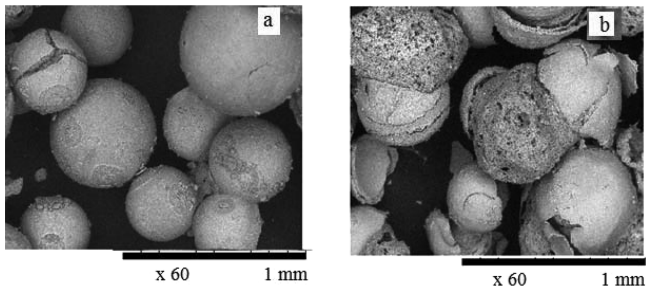

Figure 4. Micrographs of samples (a: step heat treatment; b: annealing at 800 °C).

material surface. According to a specific surface area (S_{sp}) of 110 m^2/g, a total pore volume of 0.48 cm^3/g, and an average pore size of 15−26 nm, the resulting material had a high surface porosity, which is favorable for practical applications.

Acid−Base Properties. In a previous work, the acid−base properties of the surface of the samples dried at 60 °C and annealed at 600 and 800 °C were studied to determine the surface charge of the material.[45]

Changing the pH of the suspension of samples dried at 60 °C was due to the dissolution of calcium ions as they were still part of the soluble nitrates. Since the calcium ion exhibited strong basic properties, the pH of the sample suspension was weakly acidic (pH = 6). Also, on the surface of the samples, there are various acid and basic centers, e.g., Ti^{4+}, Si^{4+} (Lewis acid centers), −OH groups (Brønsted basic centers), Si−O−Si, and Ti−O−Ti (Lewis basic centers).

Regardless of the temperature treatment of the samples, the pH value increased sharply up to 10, indicating that the sample is a Brønsted base; the mechanism of adsorption is shown in Figure 5. This surface charge affects the distribution of ions near it when immersed in SBF. It was found that, during the

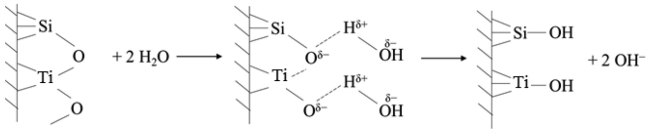

Figure 5. Adsorption mechanism.

first 10 s, the desorption of the hydroxyl-hydrate cover from the air occurs due to which the pH of the suspension increases sharply. After 16 min, the pH value stabilizes in the range from 10 to 11; this indicates that the surface of the samples is a base. Since Si−OH bonds are not identified in the samples calcined at 800 °C, according to IR spectroscopy data, the surface represents the Lewis base center. Meanwhile, in the solution, the samples' main centers interact with the protons of water molecules. The remaining less strongly bonded hydroxo-groups of water passed into the solution, causing the basicity of the medium to increase dramatically. After the surface interacted with the aqueous solution, the surface became a Brønsted base.

Biomimetic Properties. The resulting material is characterized by a regular structure with a spherical particle shape (Figure 6a,b) TiO_2-SiO_2; the framework is uniformly fixed on the cationite (Figure 6c). Figure 6d shows a cross section of the obtained material and a map of element distribution (Figure 6f). The figure shows that the main element of the inner part of the sphere is calcium, with a small inclusion of other elements. Furthermore, the main elements of the outer framework are titanium and silicon, with a small inclusion of calcium. Thermal treatment of hybrid mesostructures leads to the formation of mesoporous materials with a specific regular structure in the nanometer range and highly developed surface, which is important for fixation of biological cells on the surface of materials when introduced into the biosphere.

One of the key problems in the creation of biofabrics is the development of two- and three-dimensional matrices or frameworks. The range of biodegradable polymeric materials is quite wide: alginates, collagen, gelatin, and saturated α-hydroxy acid derivatives—polyoxyalkanoates including polymers of lactic and glycolic acids (polylactides and polyglycolides), poly(ε-caprolactone), sodium silicate (liquid glass), polyvinyl alcohol as well as polyesters of bacterial origin (poly-β-oxybutyrate and its copolymers with oxyvalerate), hyaluronic acid, aliphatic polyesters, etc. The choice of the material depends on the functional purpose of the constructed bio-artificial tissue; as such, properties like mechanical strength, elasticity, biocompatibility, degradability, and porosity affect the ability to support cell attachment, growth, proliferation, and differentiation. In this study,

https://doi.org/10.1021/acsomega.1c02918
ACS Omega 2021, 6, 21104−21112

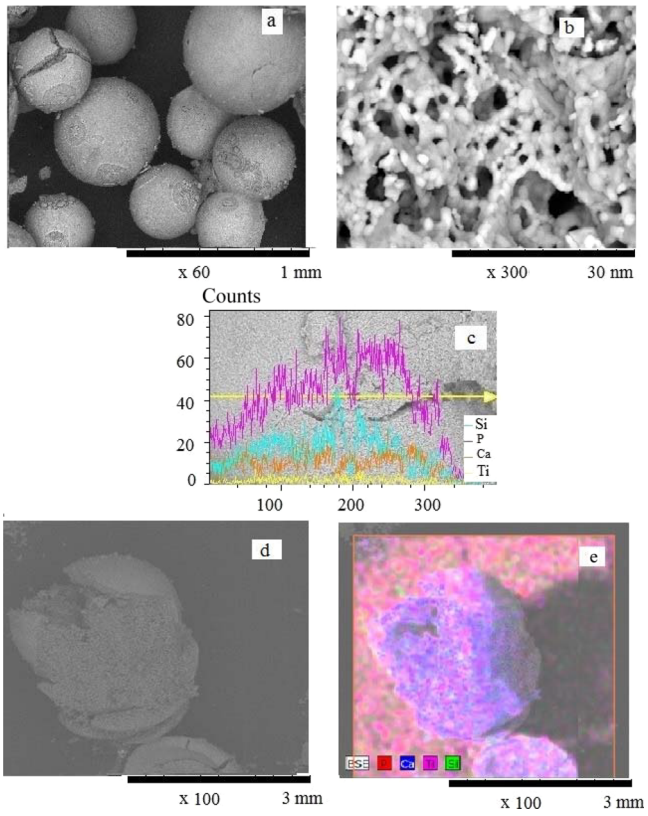

Figure 6. Microphotographs of the sample surface ((a) magnification of 60, (b) magnification of 3000, and (d) magnification of 100), distribution of elements along the line (c), and elemental distribution map (e).

polyvinyl alcohol (PVS), gelatin, and sodium silicate (liquid glass) were chosen as binding additives to create a three-dimensional framework.

Biomimetic studies of the samples were carried out in a model SBF (simulated body fluid) solution.[48] When the material reacts with the aqueous solution, both chemical and structural changes occur on the surface as a function of time, leading to changes in the pH of solutions.[40,41,48] Figure 7 shows the time dependence of the change in pH of physiological SBF solution with samples immersed in it.

As soon as the samples were immersed in physiological solution, there was a rapid increase in pH in the first day, and then the increase was not so significant. The increase in pH

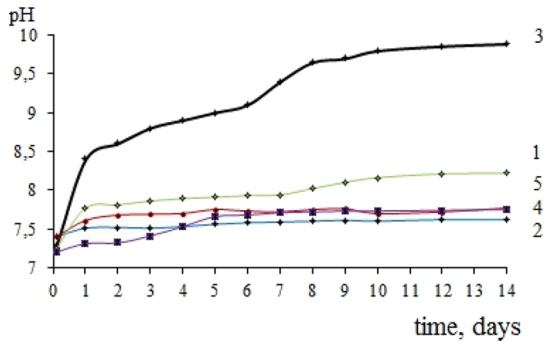

Figure 7. Dynamics of pH change of physiological solution with the samples under study: 1, without binder; 2, liquid glass; 3, PVS freezing; 4, PVS annealing; 5, gelatin.

created a favorable atmosphere for crystallization of the calcium-phosphate layer on the surface of the material.[40,41] The rapid release of alkaline and alkaline-earth ions from the solution as well as the increase in pH testifies to the high reactivity of the studied samples. The formation of a calcium-phosphate layer on the bioactive materials and the migration of soluble silicon and calcium ions into the surrounding tissues are key factors for the rapid binding of these materials to the tissue.

However, the high pH value = 10, when using liquid glass as a binder, is not favorable for calcium-phosphate mineralization on the material surface. According to the form of kinetic curves ($C(Ca^{2+}$ and $Mg^{2+})$, mmol/L$-\tau$, day), the process of accumulation of compounds containing calcium and magnesium ions on the material surface (Figure 8 and Table 3) can be divided into three stages. Adsorption of Ca^{2+} and Mg^{2+} ions from SBF solution at the first stage (up to 3 days) is the same.

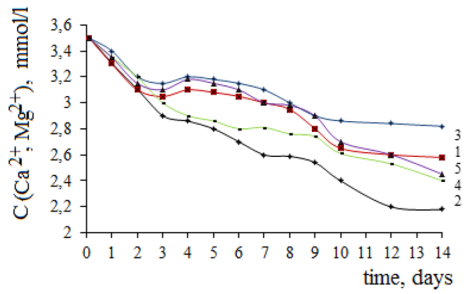

Figure 8. Accumulation curves for Ca^{2+} and Mg^{2+} ion accumulation on the surface of the biomaterial in SBF solution: 1, without binder; 2, liquid glass; 3, PVS freezing; 4, PVS annealing; 5, gelatin.

Table 3. Rate of Accumulation of Ca^{2+} and Mg^{2+} Ions in the Samples

sample	binding additive	k (0−3 days)	k (4−9 days)	k (10−14 days)
1	without binder	1.68	0.61	1.42
2	liquid glass	1.65	0.45	1.13
3	PVS freezing	1.65	0.50	1.31
4	PVS annealing	1.67	0.47	1.25
5	gelatin	1.66	0.51	1.29

The difference in the rate of accumulation of calcium and magnesium ions on the surface was noticeable only after 9 days (step 3).

Calcium and magnesium ions are more slowly adsorbed to the surface of sample 2 (binder liquid glass) than sample 1 (without binder). This may be due to increased acidic properties and the appearance of interfacial boundaries, resulting in an increased rate of diffusion and adsorption of counterions from the SBF solution onto the sample. The highest rate of accumulation of Ca^{2+} and Mg^{2+} ions after 14 days was observed in the sample without a binder. Among the samples with binder additives, the highest rates of accumulation were demonstrated by sample 3 (freezing binder PVA) and sample 5 (binder gelatin).

The formation of the calcium-phosphate layer on the surface of the materials occurs during 14 days of exposure in SBF solution. After 14 days of exposure, the surface of the samples becomes more friable with a large number of formed particles of round shape with sizes up to 8 μm (Figure 8). After 14 days in SBF solution, the amount of calcium phosphates on the surface of the samples increases (Figures 9 and 10). Deposition

https://doi.org/10.1021/acsomega.1c02918
ACS Omega 2021, 6, 21104−21112

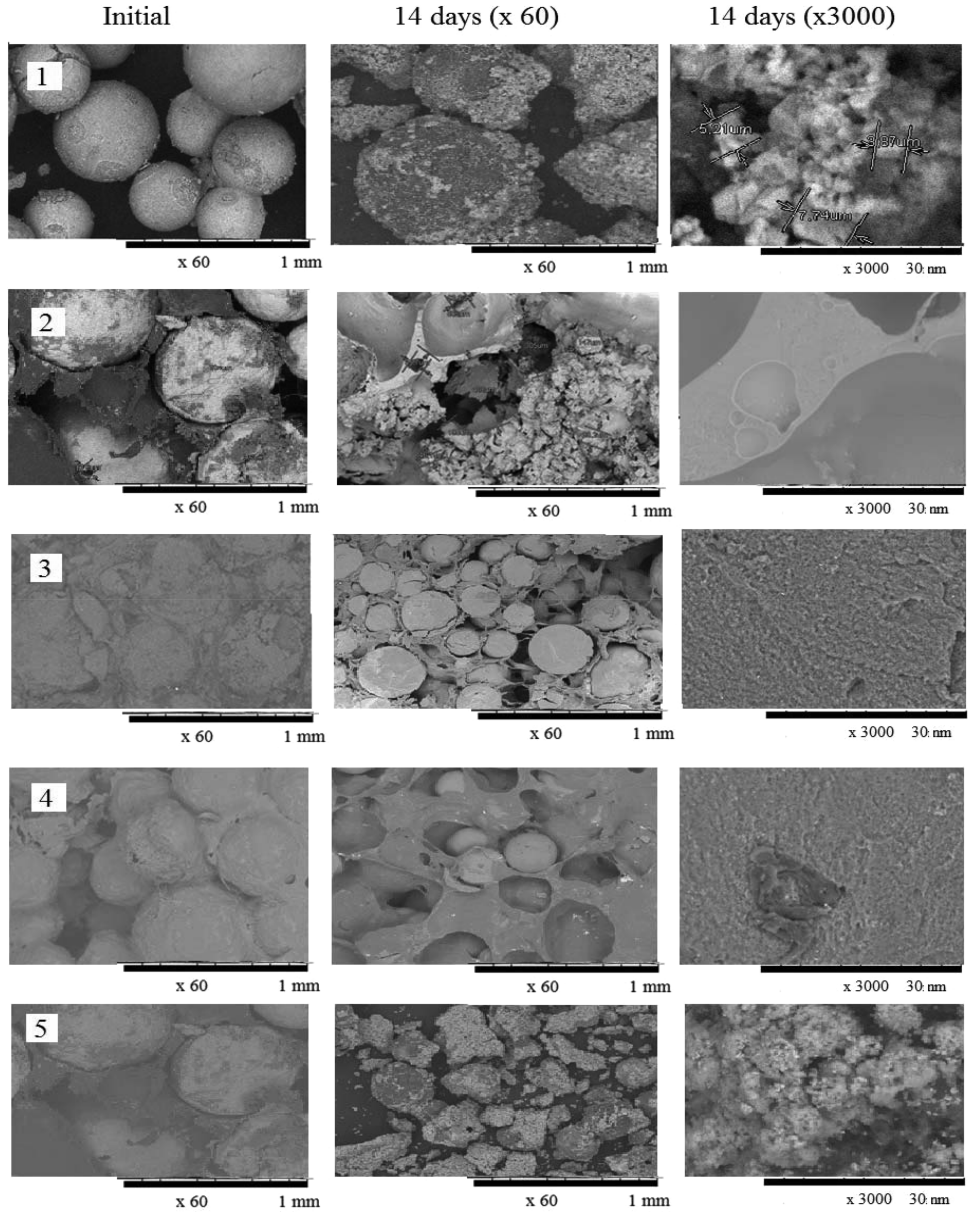

Figure 9. Microphotographs of sample surfaces showing the growth dynamics of the calcium-phosphate layer: 1, without binder; 2, liquid glass; 3, PVS freezing; 4, PVS annealing; 5, gelatin.

of various ions from SBF solution on the surface of samples occurs uniformly (Figure 9). The most uniform depositions of particles with a large number of open pores are observed in sample 1 (without additive) and sample 5 (binding additive gelatin). This topography determines the best bioactive properties due to the fact that the pores create conditions for strong adhesion to the bone tissue.

The highest concentrations of calcium ions are in sample 1 (without binder) and in sample 5 (binding gelatin) (Figure 11). Both the absolute surface content of phosphorus and calcium ions and their ratio play an important role (Table 4).

The highest values of the Ca/P ratio are in sample 1 (without binder) and in sample 5 (binder gelatin). Thus, it is acceptable to use gelatin as a binder because highly porous loose particles are formed on the surface of the samples; the bioproperties of the material and its surface composition are not changed.

CONCLUSIONS

In this study, biomaterials with a spherical particle shape based on Tokem-200 were synthesized by the sol−gel method. The framework of the material is TiO_2-SiO_2, and the inner part is filled with Ca^{2+} (sample TiO_2-SiO_2/CaO) with mol % TiO_2-65, SiO_2-30, and P_2O_5-5.

It was found that the solutions are suitable for the preparation of materials up to 5 days. A step heat treatment (after drying at 60 °C) at 150, 250, and 350 °C, each for 30 min, at 600 °C for 6 h, and 800 °C for 1 h was required to obtain the homogeneous material. Tokem-200 specimens with Ca^{2+} and applied ash have high biological activity as the surface contains active centers (Si^{4+} and Ti^{4+}) that promote mineralization and precipitation of calcium-phosphate crystals on the surface of materials in biological media. As a binding additive for binding spherical particles to each other when introduced into a biological medium, it is acceptable to use

https://doi.org/10.1021/acsomega.1c02918
ACS Omega 2021, 6, 21104−21112

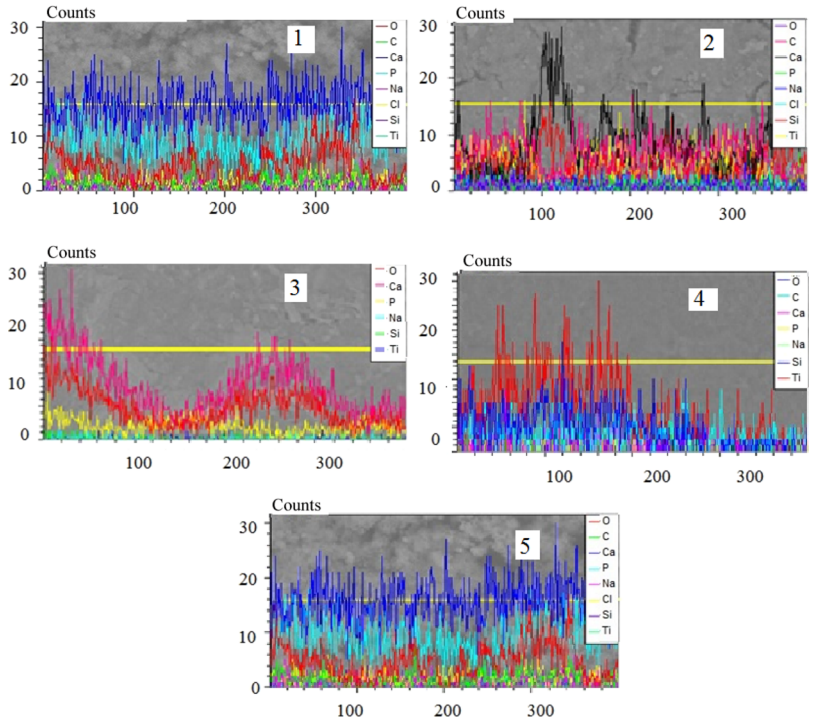

Figure 10. Linear distribution of elements on the surface of samples, after immersion in SBF solution for 14 days: 1, without binder; 2, liquid glass; 3, PVS freezing; 4, PVS annealing; 5, gelatin.

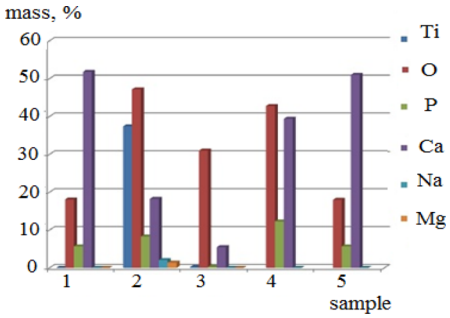

Figure 11. Elemental composition of the sample surface after immersion in SBF solution: 1, without binder; 2, liquid glass; 3, PVS freezing; 4, PVS annealing; 5, gelatin.

Table 4. Content of Calcium and Phosphorus Ions on the Surface of Samples after Immersion in SBF Solution

sample	binding additive	Ca^{2+}	$P;^{5+}$	Ca/P;
1	without binder	51	6	8.5
2	liquid glass	18	7	2.5
3	PVS freezing	5	1	5.0
4	PVS annealing	37	12	3.1
5	gelatin	50	6	8.3

gelatin since it does not affect the surface composition of the samples.

EXPERIMENTAL SECTION

Chemicals. Tetraethoxysilane (puriss. spec., Germany), orthophosphoric acid (puriss. spec. Himmed Russia), calcium nitrate (p.a. Himmed Russia), tetrabutoxytitanium (puriss. spec. Germany), and butyl alcohol were used as received from vendors.

Synthesis of Materials. The stability of the sol depends on the time required to dissolve the sol precursor (butanol-water-acid before adding the alkoxide). It is also necessary to observe the order of mixing the components when preparing the sols. To obtain biomaterials with the spherical particle shape, the sols were prepared according to the procedure described in the literature.[42]

The outer framework, the obtained materials (TiO_2-SiO_2), and the inner part were filled with Ca^{2+} (sample TiO_2-SiO_2/CaO). The calcium-containing sample of the acryl-divinylbenzene-based Tokem-200 cationite was chosen due to its high selectivity for Ca^{2+}.

To form the framework of the material, an aggregatively stable sol was prepared: solvent-butanol and acid polycondensation catalyst-phosphoric acid were mixed. A mixture of tetrabutoxytitan and tetraethoxysilane was added to the solution after C_4H_9OH-H_3PO_4 equilibrium was established. Maturation of the sols was carried out at room temperature for 3 days.

Composition 1: TiO_2 (65 mol %) - SiO_2 (30 mol %) - P_2O_5 (5 mol %).

Composition 2: TiO_2 (55 mol %) - SiO_2 (30 mol %) - P_2O_5 (15 mol %).

Composition 3: TiO_2 (45 mol %) - SiO_2 (30 mol %) - P_2O_5 (25 mol %).

Tokem-200 specimens with Ca^{2+} were immersed in the aggregatively stable sol for 12 h followed by extraction and drying at 60 °C for 60 min. After drying, the samples were subjected to a stepwise heat treatment at 150, 250, and 350 °C for 30 min each, at 600 °C for 6 h, and 800 °C for 1 h.

Introduction of binder additives was as follows:

1) Addition of liquid glass: liquid glass in a 1:1 ratio was added to dried samples of Tokem-200 with Ca^{2+} and applied sol, and then the samples were subjected to stepwise heat

https://doi.org/10.1021/acsomega.1c02918
ACS Omega 2021, 6, 21104−21112

treatment (at 150, 250, and 350 °C for 30 min each, at 600 °C for 6 h, and 800 °C for 1 h).

2) Polyvinyl alcohol (PVA) addition: PVA was added to dried samples of Tokem-200 with Ca^{2+} and applied sol in a 1:1 ratio, then some samples were subjected to stepwise heat treatment (at 150, 250, and 350 °C for 30 min each, at 600 °C for 6 h, and 800 °C for 1 h), and some samples were frozen.

3) Gelatin addition: after a stepwise heat treatment (at 150, 250, and 350 °C for 30 min each, at 600 °C for 6 h, and 800 °C for 1 h), gelatin was added to the samples in a 1:1 ratio.

Characterization. To study the film-forming ability of the solutions, the viscosity was measured with a glass viscometer (with a capillary diameter of 0.99 mm at a temperature of 25 °C). Thermal stability in an atmosphere of air of solutions dried at 60 °C was studied with a synchronous thermal analyzer STA 449 C Jupiter in an oxygen atmosphere by the shape of the TG and DSC curves in the temperature range of 60−900 °C.

The IR spectra of the dried film-forming solutions were taken on a Nicolet 6700 FTIR spectrometer in the frequency range of 4000−400 cm^{-1}. The structure (scanning electron microscopy, SEM) and chemical composition (energy-dispersive X-ray analysis, EDX) of the samples were analyzed on a Hitachi TM-3000 scanning electron microscope with a Quantax-70 attachment for energy-dispersive microanalysis. The specific surface area (S_{sp}), volume, and pore size of the powders were measured by nitrogen adsorption followed by degassing at a pressure of ∼0.1 Pa at 200 °C for 1 h on a TriStar II Micromeritics device using the Brunauer−Emmett−Teller (BET) method. A low-temperature nitrogen vapor sorption method has a relative error Δ ± 10%. The particle size (d) of the dispersed samples was estimated by the value of the specific surface area and measured pycnometric density of the powders.

The biological properties of the materials were carried out with simulated body fluid (SBF).[48] The samples were immersed in the SBF solution for 14 days with continuous temperature control at 37 °C, after which the surface morphology of the obtained materials was examined on a Hitachi TM-3000 scanning electron microscope with the Quantax-70 attachment for energy-dispersive microanalysis. The rate of calcium phosphate layer formation on the surface of substrates was assessed by the decrease in total concentration of calcium and magnesium ions ($C(Ca^{2+}$ and $Mg^{2+})$, mmol/L) in the SBF solution, determined by the trilonometric titration. The coefficient of ion accumulation Ca^{2+} and Mg^{2+} was calculated by the formula $k = \frac{C(Ca^{2+} \text{ and } Mg^{2+})}{\tau}$, where $C(Ca^{2+}$ and $Mg^{2+})$ (mmol/L) is the total change in concentration over the time interval τ (days).

AUTHOR INFORMATION

Corresponding Author

Yu-Wen Chen − *Department of Chemical Engineering, National Central University, Chung-Li 32001, Taiwan;* orcid.org/0000-0002-8519-2595; Email: ywchen@cc.ncu.edu.tw

Authors

Vladimir V. Kozik − *National Research Tomsk State University, Tomsk 634050, Russia*

Lyudmila P. Borilo − *National Research Tomsk State University, Tomsk 634050, Russia*

Ekaterina S. Lyutova − *National Research Tomsk State University, Tomsk 634050, Russia*

Complete contact information is available at: https://pubs.acs.org/10.1021/acsomega.1c02918

Notes

The authors declare no competing financial interest.

ACKNOWLEDGMENTS

The results were obtained within the framework of the state task of the Ministry of Education and Science of the Russian Federation, project no. 0721-2020-0037.

REFERENCES

(1) Evdokimov, P. V.; Putlyaev, V. I.; Ivanov, V. K.; Garshev, A. P.; Shatalova, T. B.; Orlov, N. K.; Klimashina, E. S.; Safronova, T. V. Phase equilibria in the tricalcium phosphate-mixed calcium sodium (potassium) phosphate systems. *Russ. J. Inorg. Chem.* **2014**, *59*, 1219−1227.

(2) Dorozhkin, S. V. Bioceramics of calcium orthophosphates. *Biomaterials* **2010**, *31*, 1465−1485.

(3) Chambard, M.; Marsan, O.; Charvillat, C.; Grossin, D.; Fort, P.; Rey, C.; Gitzhofer, F.; Bertrand, G. Effect of the deposition route on the microstructure of plasma-sprayed hydroxyapatite coatings. *Surf. Coat. Technol.* **2019**, *371*, 68−77.

(4) Rodrigues, L. F., Jr.; Tronco, M. C.; Escobar, C. F.; Rocha, A. S.; Santos, L. A. L. Painting method for hydroxyapatite coating on titanium substrate. *Ceram. Int.* **2019**, *45*, 14806−14815.

(5) Harun, W. S. W.; Asri, R. I. M.; Alias, J.; Zulkifli, F. H.; Kadirgama, K.; Ghani, S. A. C.; Shariffuddin, J. H. M. A comprehensive review of hydroxyapatite-based coatings adhesion on metallic biomaterials. *Ceram. Int.* **2018**, *44*, 1250−1268.

(6) Rahmani, F.; Es-Haghi, A.; Hosseini, M.-R. M.; Mollahosseini, A. Preparation and characterization of a novel nanocomposite coating based on sol-gel titania/hydroxyapatite for solid-phase microextraction. *Microchem. J.* **2019**, *145*, 942−950.

(7) Stango, S. A. X.; Vijayalakshmi, U. Synthesis and characterization of hydroxyapatite/carboxylic acid functionalized MWCNTS composites and its triple layer coatings for biomedical applications. *Ceram. Int.* **2019**, *45*, 69−81.

(8) Samavedi, S.; Whittington, A. R.; Goldstein, A. S. Calcium phosphate ceramics in bone tissue engineering: A review of properties and their influence on cell behavior. *Acta Biomater.* **2013**, *9*, 8037−8045.

(9) Sadat-Shojai, M.; Khorasani, M.; Dinpanah-Khoshdargi, E.; Jamshidi, A. Synthesis methods for nanosized hydroxyapatite with diverse structures. *Acta Biomater.* **2013**, *9*, 7591−7621.

(10) Bohner, M. Calcium orthophosphates in medicine: from ceramics to calcium phosphate cements. *Injury* **2000**, *31*, 37−47.

(11) Zhang, J.; Liu, W.; Schnitzler, V.; Tancret, F.; Bouler, J.-M. Calcium phosphate cements for bone substitution: Chemistry, handling and mechanical properties. *Acta Biomater.* **2014**, *10*, 1035−1049.

(12) Dorozhkin, S. V. Calcium orthophosphates in dentistry. *J. Mater. Med.* **2013**, *24*, 1335−1363.

(13) Hench, L.; Jones, R. *Biomaterials, artificial organs and tissue engineering*; Woodhead Publishing: Cambridge, 2005).

(14) Choi, A. H.; Ben-Nissan, B. Applications of hydroxyapatite nanocoatings and nanocomposite coatings in dentistry. *JSM Dent. Surg.* **2016**, *1002*, 1−3.

(15) Biernat, M.; Jaegermann, Z.; Tymowicz-Grzyb, P.; Konopka, G. Influence of low-temperature reaction time on morphology and phase composition of short calcium phosphate whiskers. *Process. Appl. Ceram.* **2019**, *13*, 57−64.

(16) Popa, A.-C.; Stan, G. E.; Husanu, M.-A.; Mercioniu, I.; Santos, L. F.; Fernandes, H. R.; Ferreira, J. M. F. Bioglass implant-coating

interactions in synthetic physiological fluids with varying degrees of biomimicry. *Int. J. Nanomed.* **2017**, *Volume 12*, 683−707.
(17) Kukueva, E. V.; Putlyaev, V. I.; Tikhonov, A. . A.; Safronova, T. V. Octacalcium phosphate as a precursor for the fabrication of composite bioceramics. *Inorg. Mater.* **2017**, *53*, 212−219.
(18) Yamaguchi, S.; Nath, S.; Matsushita, T.; Kokubo, T. Controlled release of strontium ions from a bioactive Ti metal with a Ca-enriched surface layer. *Acta Biomater.* **2014**, *10*, 2282−2289.
(19) Pernot, F.; Zarzycki, J.; Bonnel, F.; Rabischong, P.; Baldet, P. New glass-ceramic materials for prosthetic applications. *J. Mater. Sci.* **1979**, *14*, 1694−1706.
(20) Kolekar, T. V.; Thorat, N. D.; Yadav, H. M.; Magalad, V. T.; Shinde, M. A.; Bandgar, S. S.; Kim, J. H.; Agawane, G. L. Nanocrystalline hydroxyapatite doped with aluminium: a potential carrier for biomedical applications. *Ceram. Int.* **2016**, *42*, 5304−5311.
(21) Tagaya, M.; Kobayashi, K.; Nishikawa, M. Additive effect of phosphoric acid on phosphorus-containing mesoporous silica film formation. *Mater. Lett.* **2016**, *164*, 651−654.
(22) Ferro, A. C.; Guedes, M. Mechanochemical synthesis of hydroxyapatite using cuttlefish bone and chicken eggshell as calcium precursors. *Mater. Sci. Eng.: C* **2019**, *97*, 124−140.
(23) Matinfar, M.; Mesgar, A. S.; Mohammadi, Z. Evaluation of physicochemical, mechanical and biological properties of chitosan/carboxymethyl cellulose reinforced with multiphasic calcium phosphate whisker-like fibers for bone tissue engineering. *Mater. Sci. Eng.: C.* **2019**, *100*, 341−353.
(24) Resmim, C. M.; Dalpasquale, M.; Vielmo, N. I. C.; Mariani, F. Q.; Villalba, J. C.; Anaissi, F. J.; Caetano, M. M.; Tusi, M. M. Study of physico-chemical properties and in vitro antimicrobial activity of hydroxyapatites obtained from bone calcination. *Prog. Biomater.* **2019**, *8*, 1−9.
(25) Horta, M.; Aguilar, M.; Moura, F.; Campos, J.; Ramos, V.; Quizunda, A. Synthesis and characterization of green nanohydroxyapatite from hen eggshell by precipitation method. *Mater. Today: Proc.* **2019**, *14*, 716−721.
(26) Wu, S.-C.; Hsu, H.-C.; Hsu, S.-K.; Tseng, C.-P.; Ho, W.-F. Effects of calcination on synthesis of hydroxyapatite derived from oyster shell powders. *J. Aust. Ceram. Soc.* **2019**, *55*, 1051−1058.
(27) Esmaeilkhanian, A.; Sharifianjazi, F.; Abouchenari, A.; Rouhani, A.; Parvin, N.; Irani, M. Synthesis and characterization of natural nano-hydroxyapatite derived from turkey femur-bone waste. *Appl. Biochem. Biotechnol.* **2019**, *189*, 919−932.
(28) Ebrahimi, M.; Botelho, M.; Lu, W.; Monmaturapoj, N. Synthesis and characterization of biomimetic bioceramic nanoparticles with optimized physicochemical properties for bone tissue engineering. *J. Biomed. Mater. Res., Part A* **2019**, *107A*, 1654−1666.
(29) Natale, L. C.; Rodrigues, M. C.; Alania, Y.; Chiari, M. D. S.; Vilela, H. S.; Vieira, D. N.; Arana-Chavez, V.; Meier, M. M.; Vichi, F. M.; Braga, R. R. Development of calcium phosphate/ethylene glycol dimethacrylate particles for dental applications. *J. Biomed. Mater. Res., Part B* **2019**, *107*, 708−715.
(30) Tilkin, R. G.; Mahy, J. G.; Régibeau, N.; Grandfils, C.; Lambert, S. D. Optimization of synthesis parameters for the production of biphasic calcium phosphate ceramics via wet precipitation and sol-gel process. *ChemistrySelect* **2019**, *4*, 6634−6641.
(31) Phatai, P.; Futalan, C. M.; Kamonwannasit, S.; Khemthong, P. Structural characterization and antibacterial activity of hydroxyapatite synthesized via sol-gel method using glutinous rice as a template. *J. Sol-Gel Sci. Technol.* **2019**, *89*, 764−775.
(32) Türk, S.; Altınsoy, İ.; Efe, G. Ç.; Ipek, M.; Özacar, M.; Bindal, C. Effect of solution and calcination time on sol-gel synthesis of hydroxyapatite. *J. Bionic Eng.* **2019**, *16*, 311−318.
(33) Kurniawati, R.; Hidayat, N.; Kurniawan, R. Solid-state sintering synthesis of biphasic calcium phosphate/alumina ceramic composites and their mechanical behaviors. In *IOP Conference Series: Materials Science and Engineering*; IOP Publishing: 2019; 012095.
(34) Balakrishnan, S.; Rajendran, A.; Kulandaivelu, R.; Nellaiappan, S. N. T. S. Saponin-mediated synthesis of hydroxyapatite by hydrothermal method: characteristics, bioactivity, and antimicrobial behavior. *J. Aust. Ceram. Soc.* **2019**, *55*, 953−967.
(35) Karunakaran, G.; Kumar, G. S.; Cho, E. B.; Sunwoo, Y.; Kolesnikov, E.; Kuznetsov, D. Microwave-assisted hydrothermal synthesis of mesoporous carbonated hydroxyapatite with tunable nanoscale characteristics for biomedical applications. *Ceram. Int.* **2019**, *45*, 970−977.
(36) Castro, Y.; Mosa, J.; Aparicio, M.; Pérez-Carrillo, L. A.; Vílchez, S.; Esquena, J.; Durán, A. Sol-gel hybrid membranes loaded with meso/macroporous SiO_2, TiO_2−P_2O_5 and SiO_2−TiO_2−P_2O_5 materials with high proton conductivity. *Mater. Chem. Phys.* **2015**, *149-150*, 686−694.
(37) Chrysafi, R.; Perraki, T.; Kakali, G. Sol-gel preparation of $2CaO{\cdot}SiO_2$. *J. Eur. Ceram. Soc.* **2007**, *27*, 1707−1710.
(38) Jmal, N.; Bouaziz, J. Synthesis, characterization and bioactivity of a calcium-phosphate glass-ceramics obtained by the sol-gel processing method. *Mater. Sci. Eng.: C* **2017**, *71*, 279−288.
(39) Vijayalakshmi, U.; Rajeswari, S. Trends biomaterials. *Artif. Organs* **2006**, *19*, 57.
(40) Letaïef, N.; Lucas-Girot, A.; Oudadesse, H.; Dorbez-Sridi, R.; Boullay, P. Investigation of the surfactant type effect on characteristics and bioactivity of new mesoporous bioactive glass in the ternary system SiO_2−CaO−P_2O_5: structural, textural and reactivity studies. *Acta Biomater.* **2014**, *195*, 102−111.
(41) Shamsutdinova, A. N.; Kozik, V. V. Obtaining and properties of thin films based on titanium, silicon and nickel oxides. *Chem. Sustainable Dev.* **2016**, *24*, 699−704.
(42) Paukstis, E. A.; Kozik, V. V.; Brichkov, A. S.; Shamsutdinova, A. N.; Larina, T. V.; Zharkova, V. V.; Bobkova, L. A. Pat. 2608125 RF.Bul. 2017, *2*, 10.
(43) Vijayalakshmi, U.; Rajeswari, S. Preparation and Characterization of Microcrystalfine Hydroxyapatite Using Sol Gel Method. *Trends Biomater. Artif. Organs* **2006**, *19*, 57−62.
(44) Zhang, D.; Wang, M.; Ren, G.-j.; Song, E.-j. Preparation of biomorphic porous calcium titanate and its application for preconcentration of nickel in water and food samples. *J. Mater. Sci Eng.: C.* **2013**, *33*, 4677−4683.
(45) Borilo, L. . P.; Petrovskaya, T. S.; Lyutova, E. S. Synthesis and properties of thin SiO_2−P_2O_5−CaO films. *Inorg. Mater.* **2014**, *50*, 810−816.
(46) Kozik, V. V.; Borilo, L. P.; Lyutova, E. S.; Brichkov, A. S.; Chen, L.-W.; Izosimova, E. A. Preparation of $CaO@TiO_2$-SiO_2 biomaterial with a sol-gel method for bone implantation. *ACS Omega* **2020**, *5*, 27221−27226.
(47) Yashima, M.; Sakai, A.; Kamiyama, T.; Hoshikawa, A. Crystal structure analysis of β-tricalcium phosphate $Ca_3(PO_4)_2$ by neutron powder diffraction. *J. Solid State Chem.* **2003**, *175*, 272−277.
(48) Kokubo, T.; Kushitani, H.; Sakka, S.; Kokubo, T.; Kushitani, H.; Sakka, S. Solutions able to reproduce *in vivo* surface − structure changes in bioactive glass − ceramic A-W[3]. *Biomaterials* **1990**, *24*, 721−735.

https://doi.org/10.1021/acsomega.1c02918
ACS Omega 2021, 6, 21104−21112